NANO LETTERS

Letter

Single-Molecule Devices as Scaffolding for Multicomponent Nanostructure Assembly

Xuefeng Guo, Adam Whalley, Jennifer E. Klare, Limin Huang, Stephen O'Brien, Michael Steigerwald, and Colin Nuckolls

Nano Lett., **2007**, 7 (5), 1119-1122 • DOI: 10.1021/nl070245a

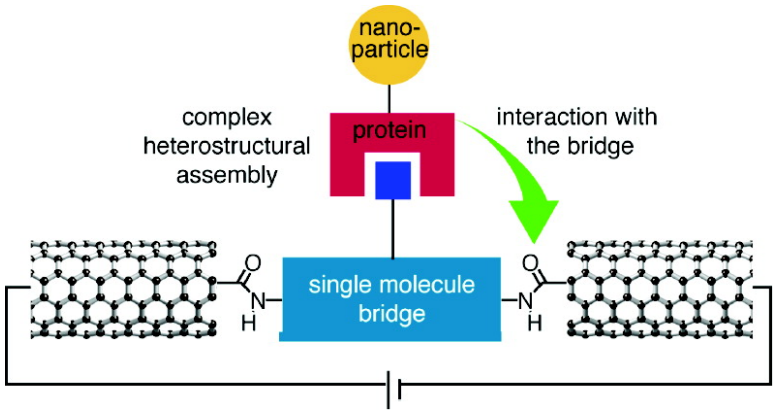

More About This Article

Additional resources and features associated with this article are available within the HTML version:

- Supporting Information
- Links to the 4 articles that cite this article, as of the time of this article download
- Access to high resolution figures
- Links to articles and content related to this article
- Copyright permission to reproduce figures and/or text from this article

View the Full Text HTML

Nano Letters is published by the American Chemical Society. 1155 Sixteenth Street N.W., Washington, DC 20036

NANO LETTERS

2007
Vol. 7, No. 5
1119−1122

Single-Molecule Devices as Scaffolding for Multicomponent Nanostructure Assembly

Xuefeng Guo,[†,‡] Adam Whalley,[†,‡] Jennifer E. Klare,[†,‡] Limin Huang,[‡,§] Stephen O'Brien,[‡,§] Michael Steigerwald,[†,‡] and Colin Nuckolls*[,†,‡]

Department of Chemistry, The Columbia University Center for Electronics of Molecular Nanostructures, and Department of Applied Physics/Applied Mathematics, Columbia University, New York, New York 10027

Received January 31, 2007; Revised Manuscript Received March 14, 2007

ABSTRACT

We report here a method to integrate discrete multicomponent assembly into molecular electronic devices. We first functionalize a molecule wired between the ends of a single-walled carbon nanotube so that it can be derivatized with a probe molecule. This probe then binds to a complementary biomolecule to form a noncovalent complex. Each step of chemical functionalization and biological assembly can be detected electrically at the single event level. Through this combination of programmed chemical reactions and molecular recognition, we are able to create complex multimeric nanostructures incorporating isolated metallic nanoparticles.

Detailed below is a method to form complex, multicomponent nanostructures from single-molecule electronic devices through the combination of programmed chemical reactivity and directed biological self-assembly. This approach forges literal and figurative connections between electrical conduction and biology that promise a future of integrated multifunctional sensors and devices.[1−9] Each device is built from an individual single-walled carbon nanotube (SWNT) that is oxidatively cut and chemically rewired together with a single conductive molecule.[10,11] Because the current flow traverses a single molecule, the devices are sensitive to the local configuration and environment around the bridging molecule. One key advantage of this approach for biosensing is the ability to form a well-defined chemical linkage between a molecular wire and a probe molecule. Moreover, because each device is constructed from a single molecule, it has the capacity to monitor individual binding events.[7] Using this approach, we are able to electrically sense oxime formation on the molecular bridge and to further detect the noncovalent binding between ligand and protein. Biological assembly within this context allows us to localize individual nanoparticles at the molecular bridge providing a means to construct and sense more complex nanostructures (Figure 1).[12]

The SWNT devices are fabricated by a method described in detail elsewhere.[10,11,13,14] This process has been optimized to give exclusively SWNTs. Figure 2A shows one of these devices with an individual SWNT spanning a set of electrodes. Initially, we electrically characterize each of the devices. The doped silicon wafer (with a 300 nm thick layer of thermally grown silicon oxide) serves as a global backgate for each of the devices. After this characterization, we oxidatively cut the tubes by means of an oxygen plasma through a nanoscale window (<10 nm) opened over the SWNTs using ultrafine electron beam lithography.[10,11] We began with 700 devices which each contain a SWNT. On the basis of the change in resistance upon cutting,[10] we determined that 166 of the original 700 devices were fully cut. Carboxylic acid functionality terminates the ends of the SWNTs after this oxidative cutting procedure.[15,16]

After removing the remaining photoresist, we reconnect the ends of the SWNT with conjugated molecules which carry amines on their ends. This process has been described in detail in a previous publication.[10] Of the 166 fully cut devices, 8 of them were reconnected with the diaminofluorenone shown in Figure 2B. As was shown in a prior study, the difference between resistance before cutting and after reconnection provides an estimate of the resistance of the bridging molecule(s).[10,17] There are two sources of variability that limit our ability to compare the electrical characteristics from device to device. One is the possibility that the gap is reconnected by more than one molecular bridge. Given the volume of the fluorenone molecule (Figure 2B) and the diameter of a standard semiconducting SWNT (6,5 SWNT $d = 0.8$ nm), it is possible to bridge with up to three

[†] Department of Chemistry.
[‡] The Columbia University Center for Electronics of Molecular Nanostructures.
[§] Department of Applied Physics/Applied Mathematics.

10.1021/nl070245a CCC: $37.00
Published on Web 03/30/2007

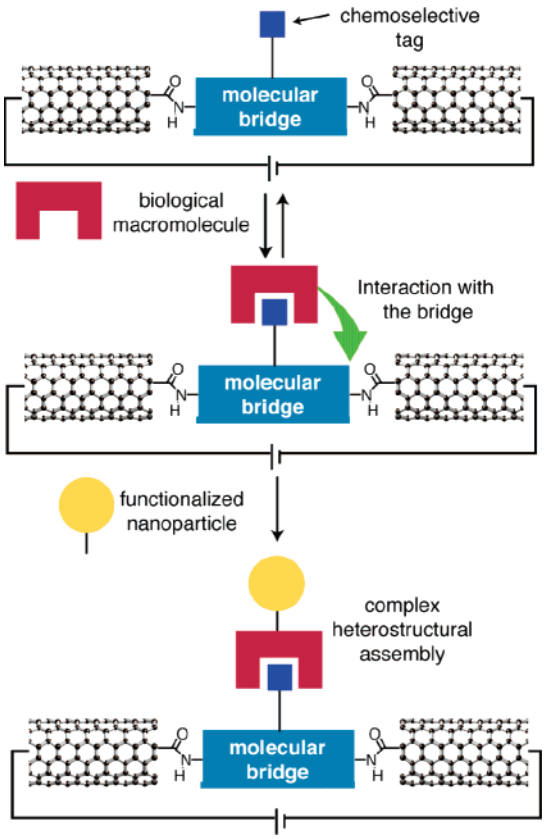

Figure 1. Schematic showing the use of single molecule electronic devices as scaffolding for assembly of biological macromolecules and complex, multimeric assemblies. The interaction of the assembly on the molecular bridge causes changes in the electrical properties of the devices.

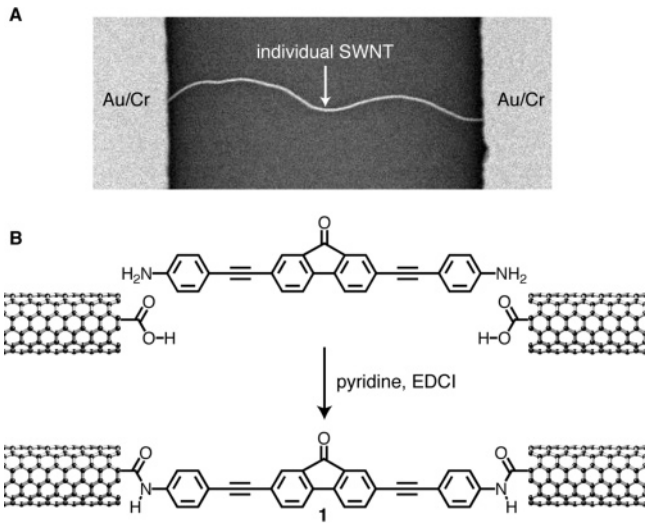

Figure 2. (A) Scanning electron micrograph of an individual SWNT device held between Au-on-Cr electrodes before it was cut and rejoined with molecules. The spacing between the electrodes is 20 μm. (B) Rejoining the ends of a cut SWNT through condensation with the diamino-substituted fluorenones to form the single molecule device **1**.

molecules. The second source of variability is the inherent variability in their electrical characteristics of the SWNTs, owing to their diameter and chirality not being well-controlled. We can exclude the possibility that the devices

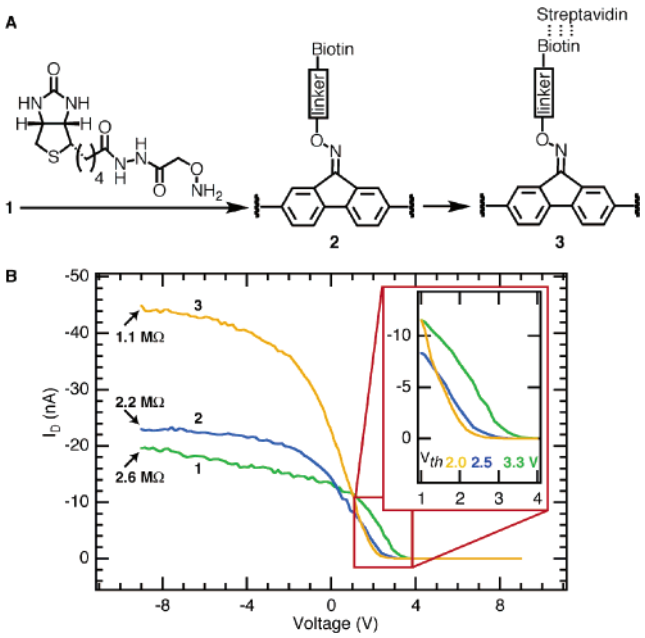

Figure 3. (A) Reaction sequence where a fluorenone is condensed with a biotin derivative that bears an alkoxyamine to form an oxime **2** on the molecular bridge. The derivatized bridge is then able to bind streptavidin to form noncovalent complex **3**. (B) Current−voltage characteristics showing the gate voltage vs the drain current at a constant source−drain voltage (50 mV) for each step in the reaction sequence.

are formed by π-stacked molecules rather than a bridging molecule because the former case has been shown to have much lower current levels.[11]

For this study, we reconnect the cut SWNT with the diaminofluorenone[18] shown in Figure 2B. It carries a ketone in the central five-membered ring that we use as a chemoselective binding site via oxime formation. Oxime formation is a mild, high-yield reaction.[19] Moreover, oximes are stable to hydrolysis[20,21] and are compatible with biological macromolecules.[22] We convert the fluorenone-based device, **1**, to the corresponding oxime-based device, **2**, by immersing it in a solution of the alkoxyamine-modified biotin derivative (1.1 mM) in pyridine (Figure 3A).[23]

We characterize the electrical properties of these devices by monitoring the current passing through them as a function of the voltage applied to the back-gate. We find that the semiconducting devices behave like p-type transistors. A comparison of the electrical characteristics of a particular device before and after oxime formation is shown in Figure 3B. Two characteristics change upon reaction: the ON-state resistance and the threshold gate voltage, V_{th}. The ON-state resistance of the ketone-based device, **1**, is higher than that of the oxime-based device, **2** (2.2 MΩ vs 2.6 MΩ), and the threshold voltage in **1** is higher (more positive) than that in **2** (3.3 V vs 2.5 V). After reaction with the hydroxylamine, seven of the eight working devices prepared above showed the same quantitative behavior as described in Figure 3; the eighth device showed extremely low current levels indicative of detachment of the bridge. Two control experiments—one where **1** was immersed in pyridine with no biotin derivative (Figure S1) and another where **1** was placed in a pyridine

solution of unmodified biotin (lacking the alkoxyamine) (Figure S2)—showed no change in ON-state resistance or threshold voltage.

The origin of the change in the ON-state resistance of these devices upon oxime formation follows recent work by Venkataraman and co-workers[24,25] on a series of arene-based molecular conductors. The conclusion of this study was that the conductance of the molecular unit varies according to its ionization potential. Specifically, phenylamines having lower ionization potentials (with all else being equal) show higher conductances. We believe that the same trend applies in the present case. We have performed density functional theory (DFT) calculations (see Supporting Information) on several fluorenones and fluorenone oximes, and in each case the energy of the HOMO (an estimate of the negative of the ionization potential) of the oxime is higher than that of the corresponding ketone. The fact that our devices behave like p-type transistors suggests that the carriers are holes. Therefore, a higher resistivity is consistent with a less easily ionized molecular subunit, and hence the oxime conducts better than the ketone.

We suggest that the shift in V_{th} between the ketone **1** and oxime **2** is due to the difference in the dipole moments of the two molecular units. DFT calculations on fluorenone and fluorenone methyl oxime show that the former has a substantially larger dipole moment than the latter (3.4 D vs 0.5 D, see the Supporting Information). In each case, the dipole lies in the plane of the molecule, pointing approximately in the direction of the C═E bond (E = O, N) with the negative end at the heteroatom. Therefore, assuming that the molecule can spin about its long axis, the field that the conduction path feels is the combination of the field due to the gate bias and the dipole field of the molecule. The effective field is less positive than the applied field, hence the apparently more positive V_{th} in the case of the molecule having the larger dipole.

We next test the ability of these biotin-tethered bridges (**2**) to recognize and bind to proteins. The functionalized devices (**2**) were then placed in a buffered solution of streptavidin, which is well-known to form a high-affinity complex.[26] The remarkable feature of the *IV* curves in Figure 3B is the drastic reduction in ON-state resistance from 2.2 to 1.1 MΩ upon association with streptavidin. We measured four devices, and the behavior in each case was the same. Silicon nanowires and intact carbon nanotubes have been previously shown to change their conductance upon biotinylation and ligation.[2,27] For the nanowires, the amount of change in conductance is typically small.[2] For the intact SWNT devices prepared by Grüner and co-workers, the mechanism for sensing is likely distinct due to the vast difference in device preparation and configuration.[27] As a point of emphasis, these large changes in resistance observed here are coming from a localized, individual probe molecule being wired into the circuit.

We have performed a number of control experiments based on the reactions above. In one set of experiments we performed the same set of reactions as detailed above but substituted bovine serum albumin (BSA) for streptavidin.

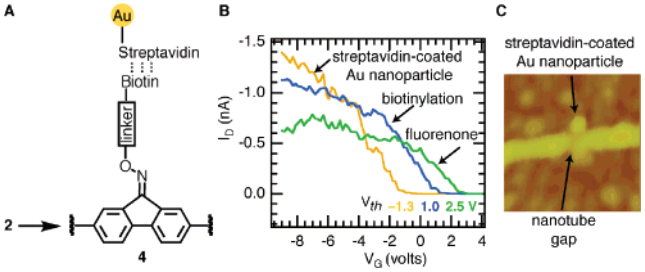

Figure 4. (A) Schematic of the biotin-tethered device binding to a ~5 nm gold nanoparticle that is coated with streptavidin. (B) Current−voltage characteristics showing the gate voltage versus the drain current at a constant source-drain voltage (50 mV) for each step in the reaction sequence. (C) AFM image of a gold nanoparticle located at the molecular junction.

BSA has no affinity for biotin and produces no measurable changes in the ON-state resistance. There is a small but significant change in the threshold voltage, possibly due to nonspecific absorption of protein. The current−voltage characteristics of these devices are contained in the Supporting Information (Figure S3). As a further control experiment, we have performed the sequence of bridging, oximation, biotinylation, and ligation with streptavidin on partially cut carbon nanotube devices (Figure S4). These are devices where the SWNT is not fully cut during the oxygen plasma treatment. There was no measurable shift of the threshold voltage for each step of the procedure. Moreover, the ON-state resistance changes before and after oximation were in opposite direction from those described above. After the devices bind with streptavidin in these control experiments, the current increases a small amount and may be due to the attachment on the partially cut positions. These results are similar to what was observed when an uncut SWNT (one which had not been exposed to an oxygen plasma) was carried through this reaction sequence (Figure S5).

What is the origin of the changes in ON-state resistance in these reconnected devices? We asserted above that the increase in conductivity between **1** and **2** is due to the increase in the energy of the HOMO of the arene bridges, and we therefore anticipate that the complexation of the streptavidin would cause an increase in the corresponding arene orbital energy. DFT calculations on the simple model system, the methyl oxime of fluorenone, have not yet shown trends that can be interpreted as the source of the orbital energy increase. Thus, systematic increases of the CNO and/or NOC bond angles and/or the CNOC dihedral angles raised the energy of the arene HOMO only slightly (1−2 mhartrees). We must conclude that the source of the increased conductivity is outside the scope of these very simple geometrical distortions that the bulky streptavidin are expected to cause.

We are able to use the programmed information of the biotin/streptavidin binding as a tool to construct more complex heterostructures from these devices. For example, we can use nanoparticles that are coated with streptavidin to localize a Au nanoparticle (~5 nm in diameter) beside the molecular junction (**4**) as shown in Figure 4A.[26] Three devices were measured and showed the same phenomenon

as in Figure 4. We see a decrease in the ON-state resistance and a large shift in the threshold voltage to more negative values. The change in ON-state resistance is smaller than the case of the streptavidin that is not bound to the nanoparticle, and the change in threshold voltage is much greater (∼0.97 to ca. −1.33 V). The increase in the magnitude of the threshold change is likely due to the greater number of proteins that are localized near the channel due to their association with the nanoparticle. The attenuation of the ON-state resistance may be due to weaker association of the particle bound streptavidin with the biotinylated bridge due to steric crowding at the point of association or a different protein environment in the streptavidin bound first to the nanoparticle. The nanoparticle also provides a means to visualize with microscopy what was inferred from the electrical data above. Figure 4C shows an AFM image of an Au particle in the gap for a device that was reconnected, tethered to the biotin derivative, and then associated with the streptavidin-modified Au particles.

In summary, we have outlined a method to introduce a hierarchy of reactivity and self-assembly in single molecule electronic devices to construct complex heterostructures. Because these heterostructures are formed in a working electrical circuit, it is possible to monitor each step in the process. First the SWNT is cut and then rejoined chemically to create the molecular electronic devices. The bridging molecule that reconnects the device is chemically programmed to form oximes, and their formation can be seen in changes in the ON-state resistance and threshold voltage for the devices. When tethered with a small molecule that binds a protein, we see large changes in the resistance in the devices. The biological assembly can be used to localize nanostructures in the junctions such as nanoparticles and points to a method to create multiterminal connections to individual molecules. Finally, because these devices are able to sense individual binding events, they make possible the formation of ultrasensitive and real-time measurements of individual binding events.

Acknowledgment. We thank Patrick Holder and Professor Matthew Francis (UC Berkeley) for insightful discussions. We also thank Philip Kim for assistance with the device characterization. We acknowledge primary financial support from the Nanoscale Science and Engineering Initiative of the National Science Foundation under NSF Award Number CHE-0117752 and by the New York State Office of Science, Technology, and Academic Research (NYSTAR) and the Department of Energy, Nanoscience Initiative (NSET#04ER46118). C.N. thanks National Science Foundation CAREER award (#DMR-02-37860) and the Alfred P. Sloan Fellowship Program (2004). We thank the MRSEC Program of the National Science Foundation under Award Number DMR-0213574 and by the New York State Office of Science, Technology and Academic Research (NYSTAR) for financial support for M.L.S.

Supporting Information Available: Details for synthetic method to synthesize the bridging molecules, the details for the rejoining and functionalization of the devices, current voltage-curves for the control experiments, and details for the DFT calculations. This material is available free of charge via the Internet at http://pubs.acs.org.

References

(1) Chen, R. J.; Bangsaruntip, S.; Drouvalakis, K. A.; Kam, N. W. S.; Shim, M.; Li, Y.; Kim, W.; Utz, P. J.; Dai, H. *Proc. Natl. Acad. Sci. U.S.A.* **2003**, *100*, 4984−4989.
(2) Cui, Y.; Wei, Q.; Park, H.; Lieber, C. M. *Science* **2001**, *293*, 1289−1292.
(3) Dai, H. *Acc. Chem. Res.* **2002**, *35*, 1035−44.
(4) Fan, R.; Karnik, R.; Yue, M.; Li, D.; Majumdar, A.; Yang, P. *Nano Lett.* **2005**, *5*, 1633−1637.
(5) Li, Y.; Qian, F.; Xiang, J.; Lieber, C. M. *Mater. Today* **2006**, *9*, 18−27.
(6) Patolsky, F.; Timko, B. P.; Yu, G.; Fang, Y.; Greytak, A. B.; Zheng, G.; Lieber, C. M. *Science* **2006**, *313*, 1100−1104.
(7) Patolsky, F.; Zheng, G.; Hayden, O.; Lakadamyali, M.; Zhuang, X.; Lieber, C. M. *Proc. Natl. Acad. Sci. U.S.A.* **2004**, *101*, 14017−14022.
(8) Patolsky, F.; Zheng, G.; Lieber, C. M. *Anal. Chem.* **2006**, *78*, 4260−4269.
(9) Zheng, G.; Patolsky, F.; Cui, Y.; Wang, W. U.; Lieber, C. M. *Nat. Biotechnol.* **2005**, *23*, 1294−1301.
(10) Guo, X.; Small, J. P.; Klare, J. E.; Wang, Y.; Purewal, M. S.; Tam, I. W.; Hong, B. H.; Caldwell, R.; Huang, L.; O'Brien, S.; Yan, J.; Breslow, R.; Wind, S. J.; Hone, J.; Kim, P.; Nuckolls, C. *Science* **2006**, *311*, 356−359.
(11) Guo, X.; Myers, M.; Xiao, S.; Lefenfeld, M.; Steiner, R.; Tulevski, G. S.; Tang, J.; Baumert, J.; Leibfarth, F.; Yardley, J. T.; Steigerwald, M. L.; Kim, P.; Nuckolls, C. *Proc. Natl. Acad. Sci. U.S.A.* **2006**, *103*, 11452−11456.
(12) Li, S.; He, P.; Dong, J.; Guo, Z.; Dai, L. *J. Am. Chem. Soc.* **2005**, *127*, 14−15.
(13) Huang, L.; White, B.; Sfeir, M. Y.; Huang, M.; Huang, H. X.; Wind, S.; Hone, J.; O'Brien, S. *J. Phys. Chem. B* **2006**, *110*, 11103−11109.
(14) Guo, X.; Huang, L.; O'Brien, S.; Kim, P.; Nuckolls, C. *J. Am. Chem. Soc.* **2005**, *127*, 15045−15047.
(15) Banerjee, S.; Hemraj-Benny, T.; Wong, S. S. *Adv. Mater.* **2005**, *17*, 17−29.
(16) Niyogi, S.; Hamon, M. A.; Hu, H.; Zhao, B.; Bhowmik, P.; Sen, R.; Itkis, M. E.; Haddon, R. C. *Acc. Chem. Res.* **2002**, *35*, 1105−1113.
(17) The values for the ON-state resistance of the devices before and after cutting are shown in Table S1 in the Supporting Information.
(18) The synthesis of the diaminofluorenone and its reactions with the cut nanotubes can be found in the Supporting Information.
(19) Freeman, J. P. *Chem. Rev.* **1973**, *73*, 283−92.
(20) Johnson, R. W.; Stieglitz, J. *J. Am. Chem. Soc.* **1934**, *56*, 1904−8.
(21) DePuy, C. H.; Ponder, B. W. *J. Am. Chem. Soc.* **1959**, *81*, 4629−31.
(22) Schlick, T. L.; Ding, Z.; Kovacs, E. W.; Francis, M. B. *J. Am. Chem. Soc.* **2005**, *127*, 3718−3723.
(23) Details for the reaction can be found in the Supporting Information.
(24) Venkataraman, L.; Park, Y. S.; Whalley, A. C.; Nuckolls, C.; Hybertsen, M. S.; Steigerwald, M. L. *Nano Lett.* **2007**, *7*, 502−506.
(25) Venkataraman, L.; Klare, J. E.; Tam, I. W.; Nuckolls, C.; Hybertsen, M. S.; Steigerwald, M. L. *Nano Lett.* **2006**, *6*, 458−462.
(26) Details for the reaction can be found in the Supporting Information.
(27) Star, A.; Gabriel, J.-C. P.; Bradley, K.; Gruener, G. *Nano Lett.* **2003**, *3*, 459−463.

NL070245A